Fibers and Polymers 2021, Vol.22, No.5, 1274-1284
DOI 10.1007/s12221-021-0560-6

ISSN 1229-9197 (print version)
ISSN 1875-0052 (electronic version)

Preparation and Characterization of Polyethylene Glycol Functional Hydroxyapatite/Polycaprolactone Electrospun Biomembranes for Bone Tissue Engineering Applications

Emre Yavuz[1,2], Ramazan Erdem[3]*, Ertan Küçüksayan[4], Esin Akarsu[1], and Murat Akarsu[1]

[1]*Department of Chemistry, Institute of Science, Akdeniz University, Antalya 07058, Turkey*
[2]*Department of Civil Engineering, Institute of Science, Akdeniz University, Antalya 07058, Turkey*
[3]*Department of Textile Technologies, Serik GSS Vocational School of Higher Education, Akdeniz University, Antalya 07500, Turkey*
[4]*Department of Medical Biochemistry, Faculty of Medicine, Alanya Alaaddin Keykubat University, Antalya 07490, Turkey*
(Received May 15, 2020; Revised July 30, 2020; Accepted August 1, 2020)

Abstract: Surfaces of previously synthesized Hydroxyapatite particles (HAP) have been modified with polyethylene glycol functional silane (PEG-400Si). For the surface modification of HAP, firstly, synthesis of PEG-400Si was performed by urethane reaction of hydroxyl and isocyanate groups. Then, HAP was synthesized by sol-gel method. Afterwards, surface modification of HAP was realized with PEG-400Si. SEM, TEM, XRD and FTIR analyses were utilized to characterize the morphology and structural properties of the synthesized and modified particles. Results revealed that the surface of HAP was modified successfully and the crystal structure of HAP was not changed after modification. Electrospinning process was conducted to obtain unmodified and modified HAP incorporated nanofibrous biomembranes and the characteristics and biological performances of these membranes have been compared to each other. SEM analysis presented that defect-free and round shape nanofibers obtained and the fiber diameter ranged from 230±114 nm to 760±291 nm. *In vitro* biological evaluations revealed that all electrospun nanofibrous biomembranes were nontoxic and the one with PCL/PEG-400Si-HAP exhibited greatest cellular protein expression approximately 1.5 times higher than the PCL biomembrane for 24 h, 48 h and 72 h.

Keywords: Hydroxyapatite, Surface modification, Electrospinning, Sol-gel, Biomembrane

Introduction

Tissue engineering is a specific research field that concentrates on developing alternative temporary biomembranes, which have the duty to replace the natural extracellular matrix (ECM) until the host cells can reform a new natural matrix [1]. Therefore, created biomembrane must enable cellular attachment, proliferation and differentiation [2]. Cells are active in a complex extracellular matrix (ECM) of pores and nanometer scale fibers [3,4]. Consequently, nanofibrous artificial biomembrane architectures with interconnective pores and large surface areas can better mimic ECM and trigger cell growth [5,6]. Recent research has also confirmed that cells could efficiently integrate and organize around the nanometer sized structures rather than their micrometer scale counterparts [7,8].

Electrospun nanofibrous membranes require substantial properties, such as considerably large surface area-to-volume ratio, high degree of porosity with a very small pore size and their 3D structure are similar to extracellular matrix. Therefore, electrospun nanofibers are reported as suitable materials for many biomedical applications, such as wound dressing, drug delivery and biomembranes for tissue engineering [9].

Electrospinning is a facile technique, which uses electrostatic forces to fabricate polymer nanofibers. Preparation of polymer fluid (solution or melt), charging of the fluid, forming the cone-jet, thinning of the instable jet in an electric field and deposition of the fibers on a collector are the characteristic stages of electrospinning process. Solution properties (viscosity, conductivity, polymer molecular weight, surface tension, polymer concentration and solvent type), process parameters (applied voltage, distance between nozzle and collector and feeding rate of the polymer solution into the system) and ambient conditions (humidity and temperature of the surroundings) are influent factors on fiber diameter and morphology during electrospinning [10].

Many tissue engineering research have been conducted to date by bringing bioceramics and biodegradable polymers together. Under the microenvironment of the organism, bioceramics exhibit splendid biological activity that can enhance new porous bone formation through self-degradation that enables cell adhesion to tissues and growth of peripheral tissues [11].

It was recorded that incorporating hydroxyapatite particles (HAP) into a polymer network enhanced the activity and viability of cell cultures on the biomembrane, buffered the acidic degradation products from the biopolymer and improved the protein absorption capacity [12-15]. However, synthesized HAP does not totally resemble to natural apatite in terms of particle morphology and composition. Furthermore, in physiological environment, polymer/HAP composites lose their strengths and integrity in the short run, and certain

*Corresponding author: ramazanerdem@akdeniz.edu.tr

failures take place at the interface of HAP and the polymer matrix as well [16]. The primary reason behind this is the inadequate integration between the ceramic phase and the polymer matrix. In order to get over this obstacle, Chio *et al*. modified the surface of HAP nanocrystals by grafting polymerization of vinyl phosphonic acid (VPA) which led to the increment in specific surface area of HAP [17]. In addition, Zhang *et al*. studied HAP/biopolymer interface interactions and they reported that silane coupling agent A174 increased the binding energy between polymer and HAP [18]. Some other previous studies also concluded that, through the surface modification of HAP by silane, it could inhibit the aggregation of HAP effectively, enhance the resistance to dissolution in acid environments, and increase interfacial bond between the HAP and polymer matrix potentially [19,20].

The surface modification can also be beneficial for cell adhesion as reported in the literature [21-23]. The particles surfaces can be modified by different organic groups such as methyl (-CH_3), amine (-NH_2), carboxylic (-COOH) and hydroxyl (-OH), etc. These modifications alter the surface chemistry of materials by changing the hydrophilicity or hydrophobicity [22-25]. Low molecular weight polyethylene glycols (PEG), a water-soluble amphiphilic polymer, exhibits unique properties such as hydrophilicity and non-toxicity which can be beneficial for selective attachment of proteins and cellular adhesion [26,27].

Many studies have been carried out in terms of developing PCL/HAP based biomembranes by utilizing different techniques such as; 3D plotting system, selective laser sintering and thermal induced phase separation technique [28-31]. Poly(e-caprolactone) (PCL) is a biodegradable, thermoplastic polyester which is frequently selected as potential biomembrane material in a variety of form for bone and cartilage repair. Due to its low glass transition temperature (-60 °C), low melting temperature (60 °C) and high decomposition temperature (350 °C), it is easy to establish polymer thermal stability in especially molten state [32].

Bone matrix proteoglycans and glycoproteins are proportionally the most abundant constituents of the noncollagenous proteins in bone matrix [33]. Therefore, we aimed to imitate bone matrix noncollagenous units with PEG functional silane modified HAP (PEG-400Si-HAP) incorporated PCL based fibrous biomembranes through electrospinning, also to evaluate these biomembranes *in vitro* to find out their suitability for bone tissue engineering applications.

Experimental

Synthesis of Polyethylene Glycol Functional Silane (PEG-400Si)

PEG-400Si was synthesized by well-known urethane reaction of hydroxyl and isocyanate groups [34]. PEG-400Si was synthesized by stirring a certain amount of 3-isocyanatopropyltriethoxysilane (IPTES) (ABCR, 95 %) and polyethylene glycol (PEG-400) (Merck, Mn:400) (1:1, molar ratio) in the presence of dibutyltin dilaurate (DBTL) (Sigma-Aldrich, 95 %) catalyst (0.01 wt.% of IPTES) under nitrogen atmosphere at 70 °C for 5 hours. The reaction mechanism is shown in Figure 1.

Synthesis of Hydroxyapatite Particles

HAP synthesis was performed using the sol-gel method with Ca/P mole ratio of 1.67 [35]. Briefly, 78.88 g of Ca $(NO_3)_2.4H_2O$ (Merck, 99-102 %) and 129.6 g of ethanol (Sigma-Aldrich, 99.5 %) were placed in 250 m*l* beaker and mixed at 500 rpm on magnetic stirrer until the solution became homogeneous. Next, pH of the solution was adjusted to 10 by adding 25 % NH_3 (Sigma-Aldrich, 28 % NH_3 in H_2O). Then, 23.2 g of $NH_4H_2PO_4$ (Merck, 99 %) and 186.5 g of distilled water (MilliQ) were placed in 500 m*l* beaker and stirred on a magnetic stirrer at 500 rpm until a homogenous solution was yielded. Following, pH of the solution was adjusted to 10 by adding 25 % NH_3. Afterwards, Calcium solution was added at a rate of 2.4 g/min over a stirring phosphate solution at 500 rpm. The resulting solution was aged at 22 hours at room temperature and centrifuged at 5000 rpm for 5 minutes. Finally, the obtained HAP was washed 6 times with distilled water, then dried under vacuum at 70 °C for 24 hours, after calcined at 750 °C for 4 hours to synthesize the white powder particles. HAP synthesis flow chart is shown in Figure 2.

Surface Modification of HAP

The surfaces of HAP were modified with the synthesized PEG-400Si. 7.5 g HAP was added into 40 m*l* toluene and was stirred for 15 min. Then 0.75 g PEG-400Si was added and stirred at 70 °C for 24 hours. After cooling to room temperature, the particles were collected by centrifuge at

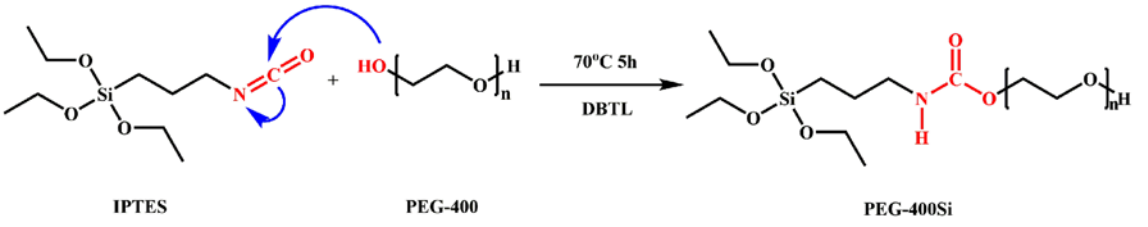

Figure 1. Synthesis reaction mechanism of PEG-400Si.

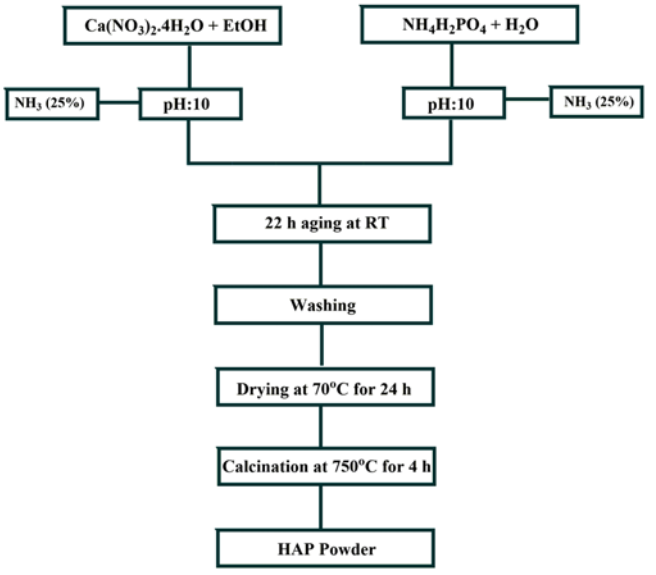

Figure 2. Flow chart of HAP synthesis.

5000 rpm for 5 min, and washed 3 times with distilled water and 3 times with ethanol, then dried with vacuum at 40 °C for 12 hours. Thus PEG-400Si-HAP were obtained. The surface modification mechanism is shown in Figure 3.

Preparation of Electrospinning Solution

PCL (MW: 80000, d:1.145 g/m*l*, Sigma-Aldrich) (9 wt.%) was dissolved in the blend of N,N-dimethylformamide (Sigma-Aldrich) (DMF)/tetrahydrofuran (THF) (Sigma-Aldrich) (70/30, v/v) by magnetic stirrer at room temperature for 6 h. Then, 2 wt. % of HAP and PEG-400Si-HAP solutions were separately prepared with DMF/THF (70/30, v/v). Next, PCL and HAP solutions were mixed at the ratio of 80/20 % (v/v) and stirred for 1 h. The preparation steps of electrospinning solution are shown in Figure 4.

Electrospinning Process

Electrospinning of nanofibrous biomembranes was performed in the laboratory spinning unit (NE200, Inovenso),

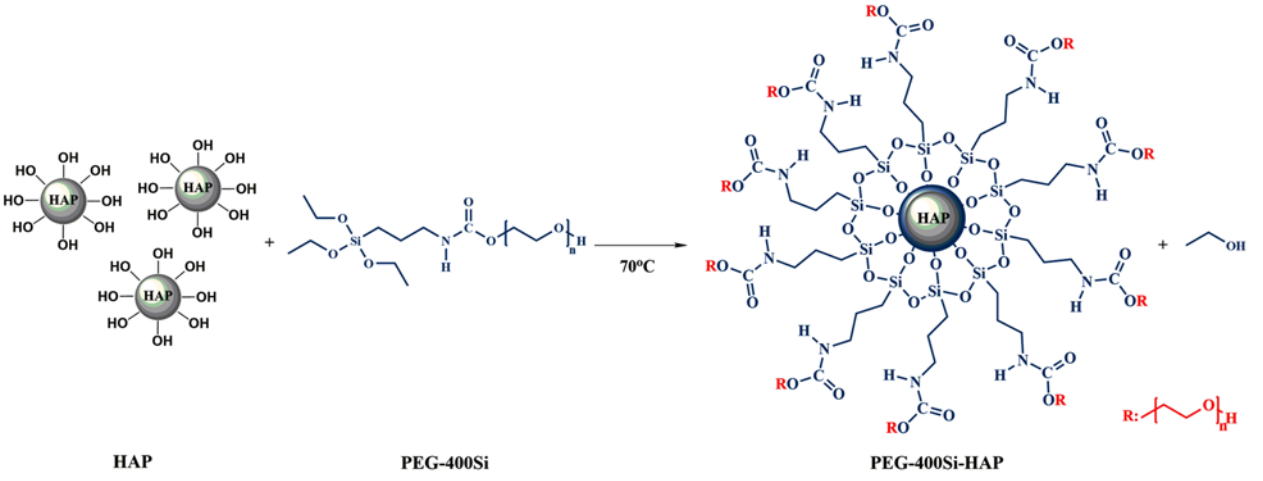

Figure 3. Surface modification mechanism of HAP with PEG-400Si.

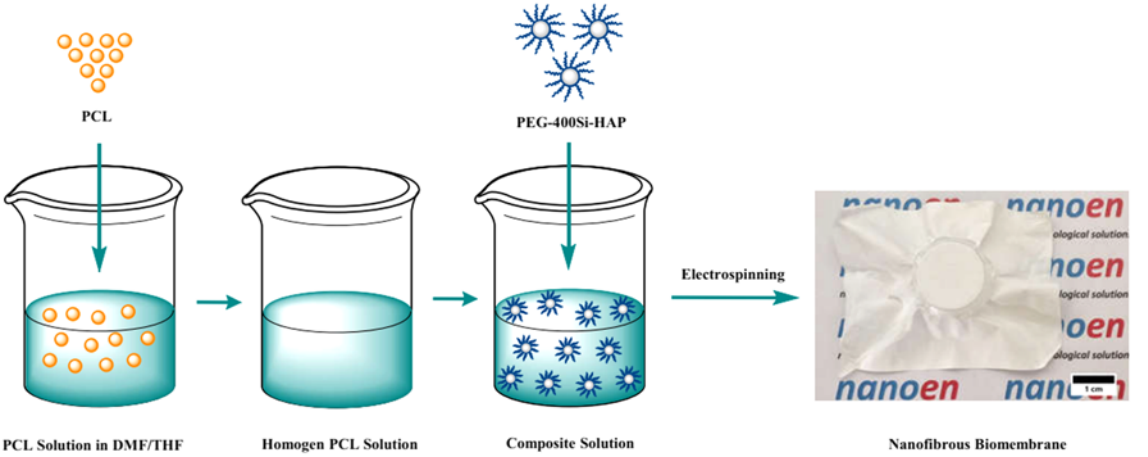

Figure 4. Schematic view of preparation of electrospinning solution and resulting electrospun nanofibrous biomembrane.

Table 1. Electrospinning parameters of each solution

Polymer	Solution amount (m*l*)	Feeding rate (m*l*/h)	Applied voltage (kV)	Distance (cm)	Drum rotation (rpm)
PCL	4	1	29	21	250
PCL/HAP	4	1.2	35	21	250
PCL/PEG-400Si-HAP	4	1	29	21	250

which has a vertical feeding apparatus (from bottom to up). Each solution was placed in a 10 m*l* syringe and sent to the drum collector (covered with aluminum foil) through a 20 gauge nozzle. Electrospinning parameters for each solution are presented in Table 1. The power supply (AC) was set up for a positive voltage between 29 kV and 35 kV. The flow rate of the solution was also determined by setting up the syringe pump in the range of 1-1.2 m*l*/h. The rotational speed of the drum collector was 250 rpm/min and its distance was set to 21 cm away from the nozzle. During the experiments, relative humidity and temperature values ranged from 43 % to 52 % RH and 24 ^{o}C to 27 ^{o}C, respectively.

Characterization of Synthesized PEG-400Si, HAP, PEG-400Si-HAP and Electrospun Fibers

Chemical analysis of PEG-400Si, HAP and PEG-400Si-HAP were performed by Fourier-transform infrared spectroscopy (FT-IR) (Bruker-Tensor 27) in transmission mode ranging from 400 to 4000 cm^{-1} at a resolution of 4 cm^{-1}. Transmittance spectra for PEG-400Si was recorded by using a horizontal attenuated total reflectance (HATR) device. In addition, HAP and PEG-400Si-HAP were analysed by using KBr pellet technique.

X-ray diffraction (XRD) analysis was performed using X-ray diffractometer (XRD, Rigaku Corp., D-MAX 2200) in the range of 20 ^{o} to 70 ^{o} with a step size of 0.02 ^{o} and speed time of 2 ^{o} per minute. Cu Kα radiations were used for measurements. Patterns were matched to patterns within The International Centre for Diffraction Data (ICDD) database.

Unmodified HAP, modified HAP and HAP incorporated electrospun fibers were characterized by scanning electron microscopy (SEM; JeolJSM 5910LV) equipped with energy dispersive spectroscopy (EDS; Oxford Instruments Inca X-Sight 7274). Samples were coated with a thin gold palladium (20/80 %) layer using a sputter coater from Polaron (SC7620) and the morphology of the structures were observed by SEM analysis at an accelerating voltage of 20 kV. Five different SEM images for each sample were analysed and 100 fibers per image were measured to calculate the average fiber diameter.

The morphology of the products particles was characterized by Transmission Electron Microscopy (TEM, ZEISS LEO906).

Viscosities of the electrospinning solutions were identified with Brookfield Digital Viscometer by using s21 type spindle with the rotational speed of 50 rpm/min. under ambient atmosphere. Five repetitions have been realized for each solution.

The electrical conductivity of the solutions was also measured with conductivity meter (WTW, Cond 3110) under ambient atmosphere. Five repetitions have been performed for each solution.

Cell Culture Studies

The cytotoxicity, cell adhesion and proliferation performances of PCL, PCL/HAP, and PCL/PEG-400Si-HAP biomembranes were determined by human osteoblast-like MG-63 cells (American Type Culture Collection, Rockville, USA). Cells were cultured in modified Eagle's minimum essential medium which was supplemented with 10 % fetal bovine serum and 1 % penicillin-streptomycin. They were grown in a humidified atmosphere containing 5 % CO_2 at 37 ^{o}C. In this study, cells were cultured with passaging 4-7 times. Cells were routinely passaged when they reached the ratio of ~80 % confluence. Finally, cells were checked with 4X, 10X and 40X lens under an inverted microscope before the experiment. Prior to cell seeding in all cell culture experiments, the substrates with biomembranes were sterilized by immersing in 70 % ethanol for 1 h followed by washing 3 times with sterilized phosphate buffered saline solution (pH=7.4, PBS). Afterwards, for further sterilization, biomembranes were placed in the plates which were exposed to UV source at the distance of 1 meter from the substitutes for 30 minutes. All chemicals and biological agents were purchased from Gibco®, Invitrogen (Carlsbad, USA) and used directly without further purification.

Trypan Blue Exclusion Test of Cell Viability

Three substrates (PCL, PCL/HAP, and PCL/PEG-400Si-HAP) were adopted to evaluate the potential of using them for biomedical applications. Trypan blue exclusion test is used to determine the number of viable cells present in a cell suspension [36]. Briefly, in order to determine the 24, 48, and 72 hours of viability, biomembranes were placed in 24 well plates. The number of seeded cells in each well was 75×10^{3}. At the end of incubation, the cells were harvested by trypsin and centrifuged. Then, cells were suspended in the 50 μ*l* medium. Next, 10 μ*l* of cell suspension and 10 μ*l* of trypan blue dye (0.4 %) were added into an eppendorf tube to obtain ½ dilution ratio. Right after, the prepared solution was mixed by pipetting up and down. Following, the solution was incubated for less than three minutes at room temperature. If the cells were dead, they appeared dark blue. In the end, approximately five minutes, the cells were counted to find out live and dead rates of the cells by utilizing

Countess, Automated Cell Counter (Invitrogen, Korea).

Quantification of Total Protein Amounts in Living Cells

Bradford method is one of the most common methods for measuring protein concentrations [37]. This method was performed to determine the total amount of protein in living cells [38]. We have focused on the increment in the amount of total protein as an indicator of viability. Briefly, in order to determine the 24, 48, and 72 hours of viability, biomembranes were placed in 24 well plates. The number of seeded cells in each well was 75×10^3. At the end of incubation, the cells were harvested by trypsin and centrifuged. By using 50 μ*l* of cell extraction buffer (Invitrogen Corporation, 542 Flynn Rd, Camarillo, CA 93012), cells were lysed in an eppendorf tubefor 10 min at +4 °C to extract their protein content for the detection processes. This buffer was containing 10 mM Tris, 2 mM Na_3VO_4, 20 mM $Na_4P_2O_7$, 100 mM NaCl, 1 mM NaF, 1 mM Egtazic acid, 1 mM ethylenediaminetetraacetic acid, 1 % Triton X-100 , 10 % glycerol, 0.1 % sodium dodecyl sulfate, 0.5 % deoxycholate, 1 mM phenylmethylsulfonyl fluoride, andprotease inhibitor cocktail at pH 7.4. Then, cell lysates were centrifuged at 14000×g at +4 °C for 10 min.

The Bradford Reagent was used to determine the concentration of proteins in cell lysates. The procedure was based on the formation of a complex between the dye, Brilliant Blue G, and proteins in cell lysates. In this method, the amount of 5 μ*l* of the cell lysates were transferred to the corresponding wells in the Protein Assay plate. 200 μ*l* of Brilliant Blue G and distilled water mixture (1:1, v/v) was also added in each related wells. Furthermore, the prepared mixtures were incubated in the Bradford Reagent plate at room temperature for at least 5 min, and then they were measured at absorbance of 595 nm by a plate reader (Multiskan™ GO Microplate Spectrophotometer). A standard cure was developed using a series of Bovine Serum Albumin (BSA) standards in the 0-32 μg/m*l* range.

XTT Cell Viability

The XTT test was used to determine the proliferation of cells and the effect of chemicals on cell viability [39]. Briefly, in order to determine the 24, 48, and 72 hours of viability, biomembranes were placed in 24 well plates. The number of seeded cells in each well was 75×10^3. At the end of incubation, the cells were harvested by trypsin and centrifuged. Then, cells were suspended in the 50 μ*l* medium which was then seeded in 96 well plates, and they were incubated at 37 °C in 5 % CO_2 for 6 hours. Then, XTT results were obtained in accordance with the manufacturer's protocol. In brief, the floating dead cells in culture medium were removed and wells were washed with 200 μ*l* of pre-warmed PBS. Then, 100 μ*l* of culture medium accompanied with 50 μ*l* of XTT solution was added to each well-plate containing cells and incubated at 37 °C in a 5 % of CO_2 containing humidified atmosphere. After 4 h incubation, percentage of cell viability was determined by recording optical absorbance at 460 nm with reference to 630 nm using a microplate reader (Multiskan™ GO Microplate Spectrophotometer). Results were normalized according to control cells.

Statistical Analysis

Biological tests were carried out by performing six of samples. Results were normalized to control group without biomembranes. Cell culture data are presented as the mean±standard error (mean±SE). Statistical analysis was performed using SPSS Data Access Pack for Windows version 23.0 (SPSS, Inc., Chicago, IL). $p\leq0.05$ was considered 95 % confidence limits as a significant difference. Categorical and continuous variables were compared using the chi-square test, ANOVA, and Student's t-test. The Mann-Whitney U-test and Kruskal-Wallis test were used to compare non-parametric variables.

Results and Discussion

Characterization of Synthesized PEG-400Si

The reaction of IPTES and PEG-400 was characterized by FT-IR spectroscopy analysis to verify of hydroxyl (-OH) and isocyanate (N=C=O) groups reaction. Figure 5 presents the FT-IR spectra of IPTES, PEG-400 and PEG-400Si. Before the reaction, IPTES, PEG have respectively reactive isocyanate and hydroxyl groups which indicated by characteristic absorption peaks of N=C=O group at 2270 cm^{-1} [40,41] and O-H group at 3450 cm^{-1} [42]. However, after the reaction between IPTES and PEG, the isocyanate's peak disappears and intensity of O-H groups is decreased. In the FT-IR spectra of the PEG-400Si exhibits new peaks appeared of carbonyl group (C=O) stretching at 1710 cm^{-1}

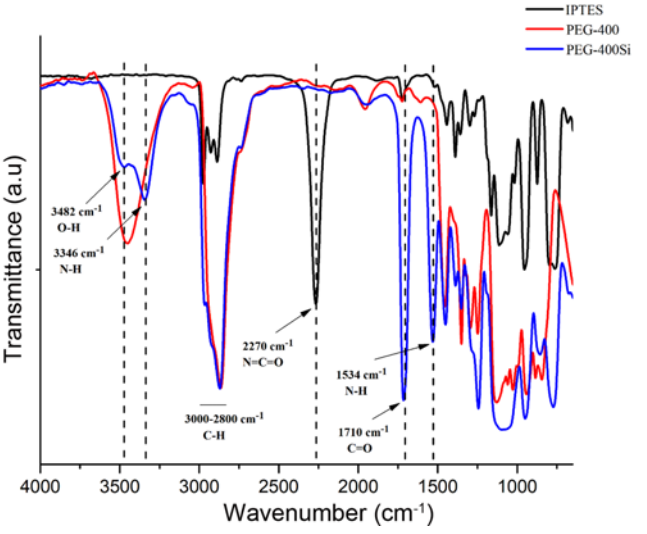

Figure 5. FT-IR spectra of IPTES, PEG-400 and PEG-400Si.

[41,42] and two bonds of secondary amine (-NHCOO-) at 3330 cm^{-1} and 1534 cm^{-1} [41,43,44]. In addition other peaks at 3000-2800 cm^{-1} [41,45] ranges C-H and 1300-1400 cm^{-1} [34] ranges C-O-H, presented bonds of PEG-400Si. These FT-IR analyses proved that the reaction between IPTES and PEG is completed and that the PEG-400Si molecule is synthesized.

Characterization of HAP and PEG-400Si modified HAP

HAP and PEG-400Si-HAP FT-IR spectra were illustrated in Figure 6. The FT-IR spectra of HAP depicts the typical functional groups of HAP. Absorption peaks at 472, 569, 602, 962, 1036 and 1093 cm^{-1} are assigned to PO_4^{-3} characteristic bands [46,47]. The two sharp peaks at 632 and 3571 cm^{-1} are indicated to hydroxyl group in crystal structure of HAP [48]. The medium band at 1634 cm^{-1} and board band at 3424 cm^{-1} are attributed to adsorbed water [47,49,50]. Small C-H stretching vibration bands appear at 2855 and 2924 cm^{-1}. The two weak peaks maybe belong to a small amount of residual organic group which comes from ethanol. In addition, three weak absorption bands of carbonate at 877, 1410 and 1460 cm^{-1} have been reported in previous studies [47,51,52]. These peaks confirm the chemical structure of HAP.

After the modification of HAP to PEG-400Si-HAP the same characteristic peaks of HAP are present in the spectrum, and new peaks appear. When HAP and PEG-400Si-HAP are compared, it is seen that PEG-400Si-HAP has characteristic absorption peaks of PEG-400Si. The emerging new bands belong to the group of carbonyl (C=O) at 1710 cm^{-1}, N-H bond at 1534 cm^{-1}, C-H bonds at 2855 and 2924 cm^{-1} and C-O-H bond at 1355 cm^{-1}. In conclusion, these observations proved that the HAP surface was successfully modified with PEG-400Si molecule.

The XRD pattern of HAP and PEG-400Si-HAP were shown in Figure 7. As can be seen, all diffraction peaks perfectly matched the standard pattern of HAP (ICDD 01-076-0694). These XRD analyses confirm that the modification of HAP does not alter the original crystal structure of the HAP.

SEM and TEM images of HAP and PEG-400Si-HAP respectively were shown in Figure 8 and Figure 9. TEM images show that the HAP and PEG-400Si-HAP particles

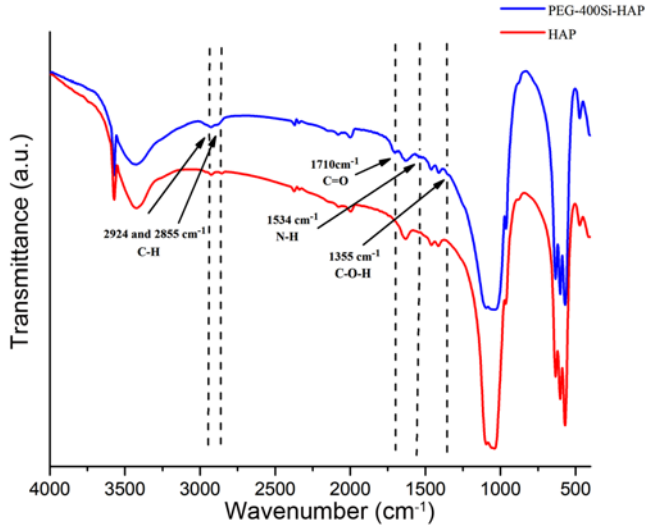

Figure 6. FT-IR spectra of HAP and PEG-400Si-HAP.

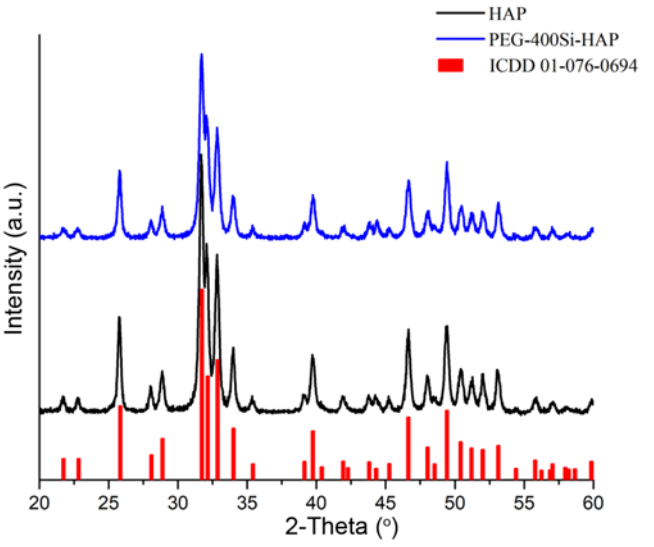

Figure 7. XRD spectra of HAP andPEG-400Si-HAP.

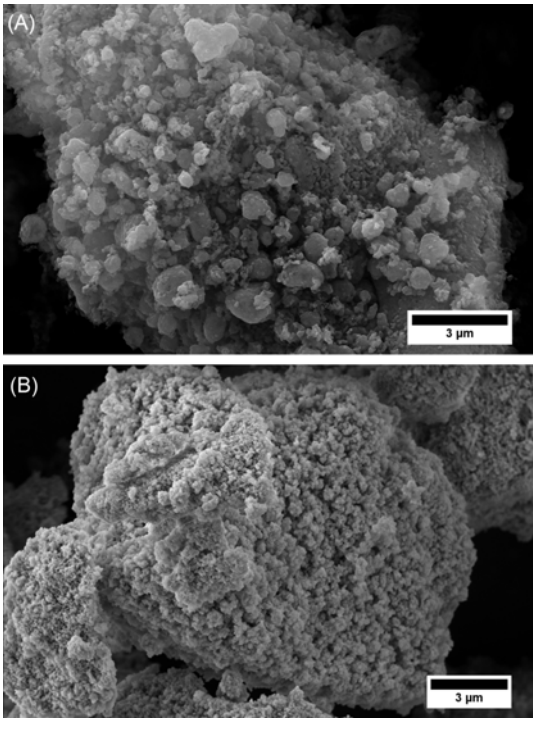

Figure 8. SEM images of particles; (A) HAP and (B) PEG-400Si-HAP.

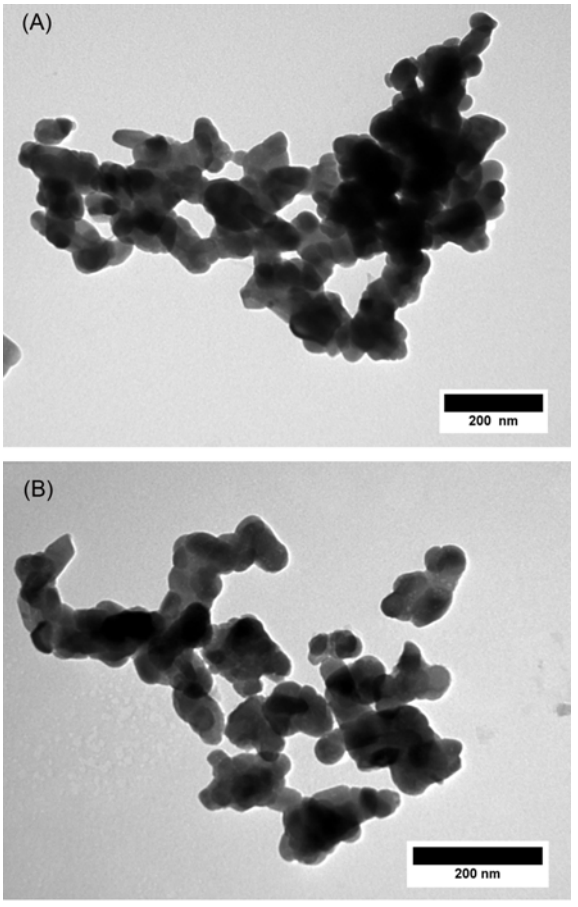

Figure 9. TEM images of particles; (A) HAP and (B) PEG-400Si-HAP.

have a nearly round shape with the average diameter range of 40-50 nm. When the HAP has been modified by the PEG-400Si molecule, the PEG-400 groups formed on the particle surfaces provided a steric effect and prevented its agglomeration of particles. It can be mentioned that from the SEM and TEM images, after surface modification of HAP, the particles are converted to highly dispersed particles.

Characterization of Nanofibrous Biomembranes

Solution properties and electrospinning parameters are two main factors that influence the final fiber characteristics during the process. In the case of solution properties, conductivity and viscosity are crucial and fundamental phenomena that significantly determine the electrospun fiber properties. The increment in the conductivity of solution produces thinner fibers during electrospinning process because the polymer solution is exposed to more stretching under the high electrical field [53]. Polymer solutions with high viscosity induce longer relaxation time for the ejected jet during electrospinning which ensures to avoid jet fracture, and also, could provoke the increase of fiber diameter [54]. In terms of process parameters, feeding rate, distance between nozzle and collector and applied voltage are vital factors to adjust fiber diameter and morphology [55].

Table 2. Solution properties and fiber diameters

Polymer	Viscosity (cP)	Conductiviy (μS/cm)	Fiber diameter (nm)
PCL	96	3.3	760±291
PCL/HAP	105	3.2	230±114
PCL/PEG-400Si-HAP	107.5	3.8	524±173

Related results about electrospinning parameters have already been presented in Table 1. On the other hand, Table 2 exhibits the solution properties and fiber diameters of pure PCL as well as the HAP added ones. According to the values, viscosities of the HAP added PCL solutions were higher than the pure PCL solution. The reason behind this finding is most probably due to the suspended HAP in the mixed solutions. In other respects, it can be stated that conductivity of the solution remained almost the same for pure PCL and PCL/HAP (3.3 μS/cm and 3.2 μS/cm, respectively); however, it barely raised for PCL/PEG-400Si-HAP solution (3.8 μS/cm), which is most probably related to the PEG-400chains on the surface of the HAP.

Figure 10 illustrates the SEM micrographs of pure PCL and HAP added PCL based nanofibrous biomembranes. It is clear that defect free and round shaped fibers have been obtained through electrospinning. For pure PCL, the measured fiber diameter was the greatest (760±291 nm). Although the viscosity of PCL/HAP solution (105 cP) was greater than the viscosity of pure PCL solution (96 cP), the yielded fiber diameter of PCL/PEG-400Si-HAP was found smaller (524±173 nm). The lowest fiber diameter was gained from PCL/HAP solution (230±114 nm), because, when the same electrospinning conditions were applied, agglomerated HAP interrupted the process. Therefore, feeding rate of the PCL/HAP solution and applied voltage had to be increased to establish fluent electrospinning which led to the dramatic decline in fiber diameter.

SEM pictures also explicitly revealed that agglomerated HAP placed on the fiber surface as well as located in the pores. In literature, it is possible to find similar studies in terms of fabricating PCL/HAP based scaffolds. For instance; Rajyer reported that nano-/micro-fibrous bioactive hybrid polycaprolactone/hydroxyapatite scaffolds were prepared by using both electrospinning and needle-punching techniques, afterwards, spherical calcium phosphate was precipitated onto the surfaces of the prepared scaffolds to prove their bioactivities. Although this study exhibits some degree of novelty, it is time consuming, labouring and not cost effective comparing with our experimental approach. Also, the level of integration between spherical calcium phosphate and the polymer remains uncertain [56]. However, in our case, PEG-400Si-HAP integrated well with the fibers as a

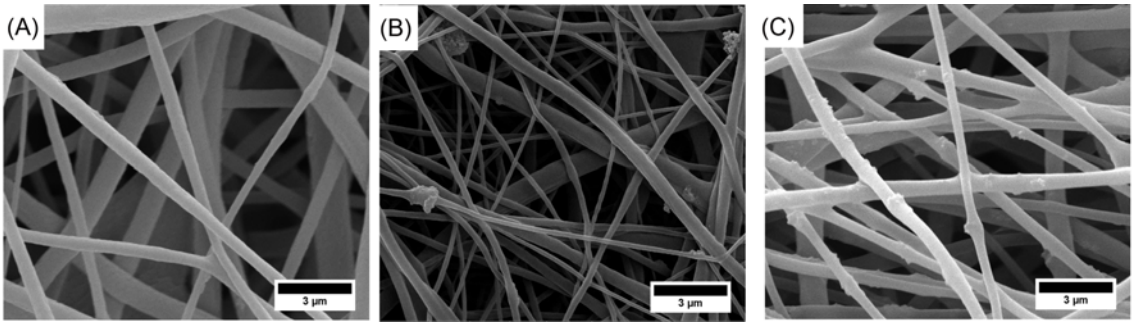

Figure 10. SEM images of pure and HAP incorporated nanofibrous biomembranes; (A) PCL, (B) PCL/HAP, and (C) PCL/PEG-400Si-HAP.

result of the surface modification of HAP, and consequently, more uniform electrospun nanofibrous biomembrane has been obtained through single process.

Trypan Blue Exclusion Test of Cell Viability

We examined the cell morphology (cell adhesion and proliferation) of human osteoblast-like MG-63 cells on PCL, PCL/HAP, and PCL/PEG-400Si-HAP biomembranes to determine the cell growth, biocompatibility and cytotoxicity of biomembranes for 24 h, 48 h, and 72 h. Findings are presented in Figure 11. It has been clearly observed that the number of cells increased in all times. Therefore, nanofibrous biomembranes were found biocompatible to cells nature. It has been noticed that the PCL/PEG-400Si-HAP biomembrane performed ideal cell proliferation compared with PCL and PCL/HAP biomembranes for 48 h and 72 h. Additionally, there was no difference among the nanofibrous biomembranes in terms of cell proliferation for 24 hours.

Quantification of Total Protein Amounts in Living Cells

As an indicator of the biocompatibility and the cell growth, we used the increase of amounts of cellular protein, the structural and vital constituent of the cell in the evaluation of biomembranes. Bradford method was applied to determine the total amount of protein in living cells for 24 h, 48 h, and 72 h and presented in Figure 12. It was found that the amount of cell protein elevated in all sample groups in all mentioned three different times. Clearly, the PCL/PEG-400Si-HAP nanofibrous biomembrane exhibited greatest cellular protein expression approximately 1.5 times higher than the PCL biomembrane for 24 h, 48 h and 72 h. Furthermore, PCL/PEG-400Si-HAP biomembrane performed ideal cellular protein expression when cell counts compared with PCL/HAP at the same time. Additionally, there was no difference in terms of cellular protein expression for 24 hours in all groups.

XTT Cell Viability

The cell proliferation and biocompatibility of the biomembranes were determined by XTT test using human osteoblast cell lines (MG-63) in Figure 13. This test is suitable for assaying cytotoxicity of our materials. PCL/PEG-400Si-HAP values were not significantly different from the control for 24 h, 48 h and 72 h. In fact, according to XTT test results, there was a decline observed in PCL and PCL/HAP biomembranes, which might be considered at first that these samples showed cytotoxic effect. However, this is not true, because this decline indicates that the rate of

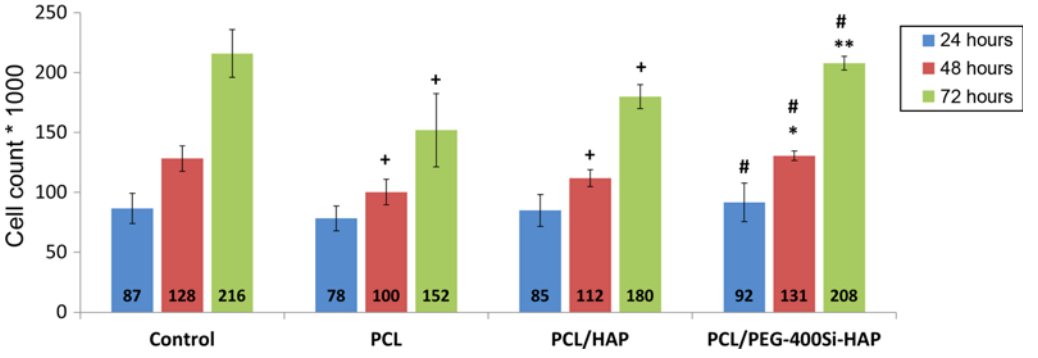

Figure 11. Effect of time-dependent cell growth of polymers with Tripan Blue assay of MG63 cells. Different modificantions of PCL increase cell growth after incubation for 24, 48, and 72 h on MG63. Each value represents mean±SE (n=6). *, $p<0.01$, PCL/PEG-400Si-HAP significantly different versus PCL and PCL/HAP for 48 h, **, $p<0.01$, PCL/PEG-400Si-HAP significantly different versus PCL and PCL/HAP for 72 h, $^{+}$, $p<0.05$, values significantly different from the control and PCL and PCL/HAP for 48 h and 72 h, $^{\#}$ $p>0.05$, values significantly no different from the control for 24 h, 48 h, and 72 h.

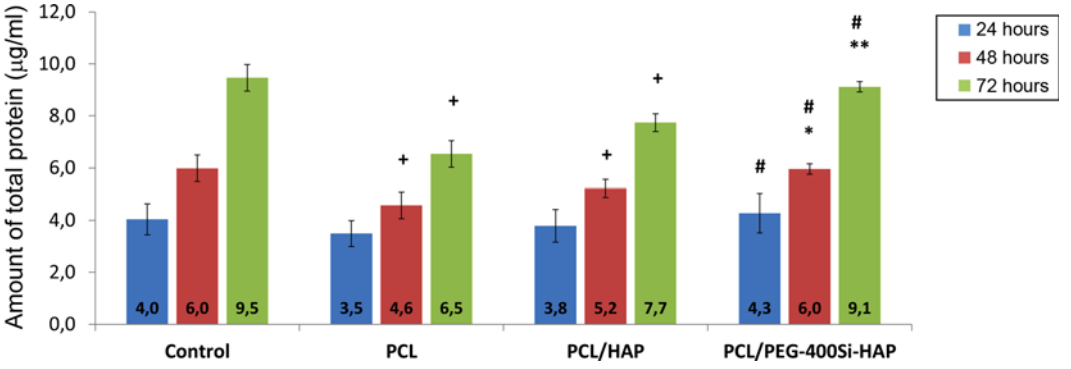

Figure 12. Effect of time-dependent total protein of polymers with Bradford assay of MG-63 cells. Different modifications of PCL increase the amount of total protein after incubation for 24, 48, and 72 h on MG63. Each value represents mean±SE (n=6). *, $p<0.01$, PCL/PEG-400Si-HAP significantly different versus PCL and PCL/HAP for 48 h, **, $p<0.01$, PCL/PEG-400Si-HAP significantly differents versus PCL and PCL/HAP for 72 h, $^{+}$, $p<0.05$, values significantly different from the control and PCL and PCL/HAP for 48 h and 72 h, $^{\#}$, $p>0.05$, values significantly no different from the control for 24 h, 48 h, and 72 h.

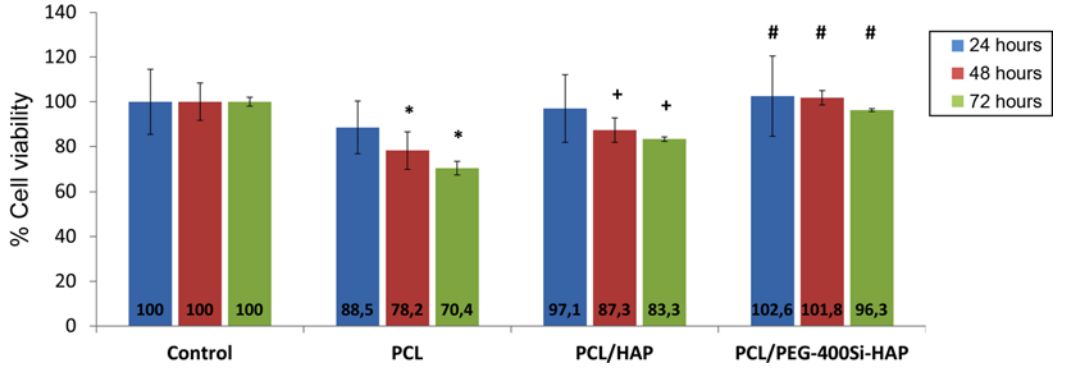

Figure 13. Effect of time-dependent cytotoxicity of polymers with XTT assay of MG63 cells. Different modificantions of PCL are normal cell viability after incubation for 24, 48, and 72 h. Each value represents mean±SE (n=6). *, $p<0.05$, PCL significantly differents versus control, PCL/HAP and PCL/PEG-400Si-HAP for 48 h and 72 h, $^{+}$, $p<0.05$, PCL/HAP significantly differents from the control and PEG-400Si-HAP for 48 h and 72 h, $^{\#}$, $p>0.05$, values significantly no different from the control for 24 h, 48 h, and 72 h.

cell proliferation decreases over time. It has been shown in previous studies that cell proliferation decreases due to increased PCL concentration [57]. In this study, we found that cell proliferation decreased in 48 and 72 hours, although we did not see changes for 24 hours by XTT test. This finding also shows that proliferation speed of cells on these membranes were slower than the cells on PCL/PEG-Si-HAP biomembranes. Therefore, PCL/PEG-400Si-HAP had a greater effect on prolonged cellular proliferation compared to PCL and PCL/HAP in XTT assay. It is evident that the added PEG-400Si-HAP into the biomembranes elevated surface hydrophilicity and the surface area, thus favoured the cellular adhesion for 24 h, 48 h, and 72 h.

Conclusion

In this study, synthesis of Polyethylene glycol functional silane (PEG-400Si) was successfully performed. Next, synthesis of hydroxyapatite particles (HAP) were also realized by utilizing sol-gel method. FTIR, XRD and SEM analysis proved that surface modification of HAP with PEG-400Si was efficiently conducted. Furthermore, by using polycaprolactone (PCL) polymer, modified and unmodified HAP incorporated nanofibrous biomembranes were smoothly fabricated through electrospinning technique. Biological evaluations proved that electrospun nanofibrous biomembranes were not accepted as toxic materials by the osteoblastic cells. PCL/PEG-400Si-HAP biomembrane exhibited the best performance in terms of biocompatibility. Especially, PEG modified HAP particles played a crucial role for cell proliferation and growth. Experimental studies proved that PCL/PEG-400Si-HAP electrospun biomembrane could be the potential scaffold candidate for bone tissue engineering applications.

Acknowledgements

Authors would like to thank to Prof. Dr. Ertuğrul Arpaç

and his Sol-Gel research group at the Chemistry Department of Akdeniz University for their great support during the experimental stage of this study. This project was funded by Akdeniz University with the project code: FBG-2019-5005.

References

1. R. Erdem, M. Yüksek, E. Sancak, O. Atak, M. Erginer, L. Kabasakal, and A. Beyit, *J. Text. Inst*., **108**, 935 (2016).
2. J. P. Vacanti and R. Langer, *The Lancet*, **354**, S32 (1999).
3. H. S. Koh, T. Yong, C. K. Chan, and S. Ramakrishna, *Biomaterials*, **29**, 3574 (2008).
4. Z. Ma, M. Kotaki, R. Inai, and S. Ramakrishna, *Tissue Eng.*, **11**, 101 (2005).
5. X. Liu, Y. Won, and P. X. Ma, *Biomaterials*, **27**, 3980 (2006).
6. K. M. Woo, V. J. Chen, and P. X. Ma, *J. Biomed. Mater. Res. Part A*, **67**, 531 (2003).
7. E. M. Christenson, K. S. Anseth, J. J. van den Beucken, C. K. Chan, B. Ercan, J. A. Jansen, C. T. Laurencin, W. J. Li, R. Murugan, L. S. Nair, S. Ramakrishna, R. S. Tuan, T. J. Webster, and A. G. Mikos, *J. Orthop. Res.*, **25**, 11 (2007).
8. S. Liao, R. Murugan, C. K. Chan, and S. Ramakrishna, *J. Mech. Behav. Biomed. Mater.*, **1**, 252 (2008).
9. R. Erdem and M. Akalın, *J. Ind. Text.*, **44**, 553 (2013).
10. D. H. Reneker and I. Chun, *Nanotechnology*, **7**, 216 (1996).
11. S. Verrier, J. J. Blaker, V. Maquet, L. L. Hench, and A. R. Boccaccini, *Biomaterials*, **25**, 3013 (2004).
12. K. Zhang, Y. Wang, M. A. Hillmyer, and L. F. Francis, *Biomaterials*, **25**, 2489 (2004).
13. E. Nejati, H. Mirzadeh, and M. Zandi, *Compos. Part A: Appl. Sci. Manuf.*, **39**, 1589 (2008).
14. R. Zhang and P. X. Ma, *J. Biomed. Mater. Res*., **44**, 446 (1999).
15. R. Zhang and P. X. Ma, *Macromol. Biosci.*, **4**, 100 (2004).
16. S. M. Zhang, J. Liu, W. Zhou, L. Cheng, and X. D. Guo, *Curr. Appl. Phys*., **5**, 516 (2005).
17. H. W. Choi, H. J. Lee, K. J. Kim, H. M. Kim, and S. C. Lee, *J. Colloid Interface Sci.*, **304**, 277 (2006).
18. H. P. Zhang, X. Lu, Y. Leng, L. Fang, S. Qu, B. Feng, J. Weng, and J. Wang, *Acta Biomater.*, **5**, 1169 (2009).
19. H. Tanaka, A. Yasukawa, K. Kandori, and T. Ishikawa, *Colloids Surf. A: Physicochem. Eng. Asp.*, **125**, 53 (1997).
20. L. Borum-Nicholas and O. C. Wilson, *Biomaterials*, **24**, 3671 (2003).
21. X. Zhang, D. Zeng, N. Li, J. Wen, X. Jiang, C. Liu, and Y. Li, *Scientific Reports*, **6**, 19361 (2016).
22. B. H. Atak, B. Buyuk, M. Huysal, S. Isik, M. Senel, W. Metzger, and G. Cetin, *Carbohydr. Polym*., **164**, 200 (2017).
23. S. Rehman, K. Khan, M. Mujahid, and S. Nosheen, *Mater. Sci. Eng. C Mater. Biol. Appl.*, **58**, 675 (2016).
24. Y. Arima and H. Iwata, *Biomaterials*, **28**, 3074 (2007).
25. W. H. Tse, L. Gyenis, D. W. Litchfield, and J. Zhang, *J. Biomater. Appl.*, **31**, 1087 (2017).
26. J. H. Lee, H. B. Lee, and J. D. Andrade, *Prog. Polym. Sci*., **21**, A-3B (1997).
27. R. Williams in "Surface Modification of Biomaterials Methods Analysis and Applications", 1st ed. (A. Rhodes, S. S. Sandhu, and S. J. Onis Eds.), Chapter 2, pp.39-55, Woodhead Publishing, Cambridge, UK, 2011.
28. S. A. Park, S. H. Lee, and W. D. Kim, *Bioprocess Biosyst Eng.*, **34**, 505 (2011).
29. Y. S. Cho, S. Choi, S.-H. Lee, K. K. Kim, and Y.-S. Cho, *Eur. Polym. J*., **113**, 340 (2019).
30. F. E. Wiria, K. F. Leong, C. K. Chua, and Y. Liu, *Acta Biomater*, **3**, 1 (2007).
31. K. Szustakiewicz, M. Gazińska, B. Kryszak, M. Grzymajło, J. Pigłowski, R. J. Wiglusz, and M. Okamoto, *Eur. Polym. J*., **113**, 313 (2019).
32. P. Yilgor, R. A. Sousa, R. L. Reis, N. Hasirci, and V. Hasirci, *Macromolecular Symposia*, **269**, 92 (2008).
33. P. Gehron Robey in "Principles of Bone Biology", (J. P. Bilezikian, L. G. Raisz, and T. J. Martin Eds.), 3rd ed. p.335, Academic Press, San Diego, 2008.
34. E. Burunkaya, Ö. Kesmez, N. Kiraz, H. E. Çamurlu, M. Asiltürk, and E. Arpaç, *Thin Solid Films*, **522**, 238 (2012).
35. F. Bakan, O. Laçin, and H. Sarac, *Powder Technol.,* **233**, 295 (2013).
36. W. Strober, *Curr. Protoc. Immunol.*, **21**, A.3B.1 (2001).
37. M. M. Bradford, *Analytical Biochemistry*, **72**, 248 (1976).
38. B. Sissolak, C. Zabik, N. Saric, W. Sommeregger, K. Vorauer-Uhl, and G. Striedner, *Biotechnol. J.*, **14**, 1800714 (2019).
39. S. Gowrishankar and S. K. Pandian, *Biochim. Biophys. Acta Biomembr.*, **1859**, 1254 (2017).
40. H. Kothandaraman, A. Sultan Nasar, and R. K. Lakshmi, *J. Appl. Polym. Sci.*, **53**, 31 (1994).
41. B. H. Stuart, "Infrared Spectroscopy: Fundamentals and Application", p.123, Wiley, 2004.
42. J. Coates, *Encyclopedia of Analytical Chemistry*, 10.1002/9780470027318 (2006).
43. S. A. Guelcher, K. M. Gallagher, J. E. Didier, D. B. Klinedinst, J. S. Doctor, A. S. Goldstein, G. L. Wilkes, E. J. Beckman, and J. O. Hollinger, *Acta Biomater.*, **1**, 471 (2005).
44. Q. He, J. Zhang, J. Shi, Z. Zhu, L. Zhang, W. Bu, L. Guo, and Y. Chen, *Biomaterials*, **31**, 1085 (2010).
45. F. Rubio, J. Rubio, and J. L. Oteo, *Spectroscopy Letters*, **31**, 199 (1998).
46. M. Salarian, M. Solati-Hashjin, S. S. Shafiei, R. Salarian, and Z. A. Nemati, *Ceram. Int.*, **35**, 2563 (2009).
47. Y. Sun, G. Guo, Z. Wang, and H. Guo, *Ceram. Int.*, **32**, 951 (2006).
48. R. N. Panda, M. F. Hsieh, R. J. Chung, and T. S. Chin, *J. Phys. Chem. Solids*, **64**, 193 (2003).
49. K. Lin, J. Chang, R. Cheng, and M. Ruan, *Mater. Lett.*, **61**,

1683 (2007).
50. Y. Wang, J. Chen, K. Wei, S. Zhang, and X. Wang, *Mater. Lett.*, **60**, 3227 (2006).
51. J. A. M. van der Houwen, G. Cressey, B. A. Cressey, and E. Valsami-Jones, *J. Crystal Growth*, **249**, 572 (2003).
52. F. Ren, Y. Ding, and Y. Leng, *J. Biomed. Mater. Res. A*, **102**, 496 (2014).
53. T. Lin, H. Wang, H. Wang, and X. Wang, *Nanotechnology*, **15**, 1375 (2004).
54. J. Li, A. He, J. Zheng, and C. C. Han, *Biomacromolecules*, **7**, 2243 (2006).
55. R. Erdem, M. İlhan, M. K. Ekmekçi, and Ö. Erdem, *Appl. Surf. Sci*., **421**, 240 (2017).
56. I. Rajzer, *J. Mater. Sci*., **49**, 5799 (2014).
57. S.-R. Son, N.-T. B. Linh, H.-M. Yang, and B.-T. Lee, *Sci. Technol. Adv. Mater.*, **14**, 015009 (2013).